

High-pressure structural and electronic properties of carbon

S. Fahy and Steven G. Louie

*Department of Physics, University of California, Berkeley, California 94720
and Materials and Chemical Sciences Division, Lawrence Berkeley Laboratory, Berkeley, California 94720*

(Received 15 December 1986)

The high-pressure properties of carbon in eight different structures are calculated using an *ab initio* pseudopotential local-orbital method. In particular, the structural properties of hexagonal diamond and variation of its fundamental band gap with pressure are calculated for the first time. The variation of the fundamental gap in hexagonal diamond is found to have the opposite sign to that in cubic diamond, although the cubic and hexagonal forms have almost identical structural properties. Among the structures examined, diamond is found to transform under hydrostatic pressure first to the fourfold coordinated bc-8 (or Si-III) structure. The bc-8 form is favored at pressures greater than 11.1 Mbar. This is a slightly lower transformation pressure than that recently calculated using the pseudopotential plane-wave method. The sixfold coordinated structures, simple cubic and β -tin, are found at low pressure to be kinetically unstable, transforming spontaneously, without an energy barrier, into the cubic diamond structure. This result suggests that sixfold coordination of liquid carbon will be unlikely to occur at moderate pressure and temperature. Similarly, sixfold coordination is not expected in carbon clusters. A method of fully utilizing crystal symmetry to reduce the amount of computation in evaluating two- and three-center integrals needed in the local-orbital method is developed for the present calculations.

I. INTRODUCTION

The high-pressure properties of carbon are of great theoretical interest at this time because of the enormous importance of the diamond anvil cell in high-pressure physics¹ and also in the context of structural stability and general high-pressure behavior of all semiconductors and insulators.²⁻⁶ With present techniques using the diamond anvil cell, the stability of diamond effectively imposes an upper bound on the pressures which can be statically generated in the laboratory. Thus it is of great importance to calculate as accurately as possible the general high-pressure properties of carbon.⁷⁻¹³

The combination of local-density-functional theory,¹⁴ *ab initio* pseudopotential,¹⁵ and the self-consistent local-orbital technique^{16,17} is exceptionally well suited to the study of this problem. Local-density-functional theory has been shown in the past to be capable of calculating with considerable accuracy the structural properties of a broad range of solid-state systems. Carbon, with its small core consisting only of the 1s state, is a good candidate for the *ab initio* pseudopotential approach because the core wave functions do not overlap significantly with the valence wave functions, and, moreover, the core eigenvalues are well separated from the valence eigenvalues. Although the resulting pseudopotentials are much deeper than is the case with, for instance, silicon or germanium, this does not pose serious problems in the present approach because we do not represent the pseudopotential in Fourier space. Finally, turning to the question of representation of the eigenstates in the Kohn-Sham equations,¹⁸ a relatively small local-orbital basis (12 orbitals per atom) can be used to represent with great accuracy the highly localized valence states in carbon.

In this paper we study fourfold, sixfold, eightfold, and twelvefold coordinated structures of carbon. The fourfold coordinated structures are cubic diamond, hexagonal diamond, and the bc-8 or Si-III structure.¹⁹ Simple-cubic and the β -tin structure are the sixfold coordinated structures, body-centered cubic the eightfold coordinated structure, and hexagonal close-packed and face-centered cubic the twelvefold coordinated structures. As in silicon and germanium,²⁰ the minimum energy of each structure (i.e., the equilibrium energy at zero pressure) increases with coordination number. (See Fig. 1.) The three fourfold coordinated structures are found to lie within 0.7 eV/atom of each other at zero pressure, the sixfold coordinated structures approximately 2.5 eV/atom higher, and the eight and twelvefold coordinated structures approximately 5 eV/atom above the fourfold coordinated structures.

Of the above structures, the only ones which have been observed experimentally for carbon are the cubic and hexagonal diamond forms. Cubic diamond is the common form of diamond²¹ but the hexagonal variety has been observed to occur naturally in craters formed by meteorites²² and has also been synthesized artificially from graphite.²³ Crystalline carbon also occurs in the hexagonal graphite (the most stable form at zero pressure) and rhombohedral graphite structures.²¹ Because of their low density we have not included the graphitic structures in the present study since we are concerned with very-high-pressure properties.

The calculated structural properties of cubic diamond and hexagonal diamond are almost identical, and are in excellent agreement with experiment and with previous calculations^{7-9,13,16} for cubic diamond. The difference in their equilibrium energies is only 0.03 eV/atom, hexago-

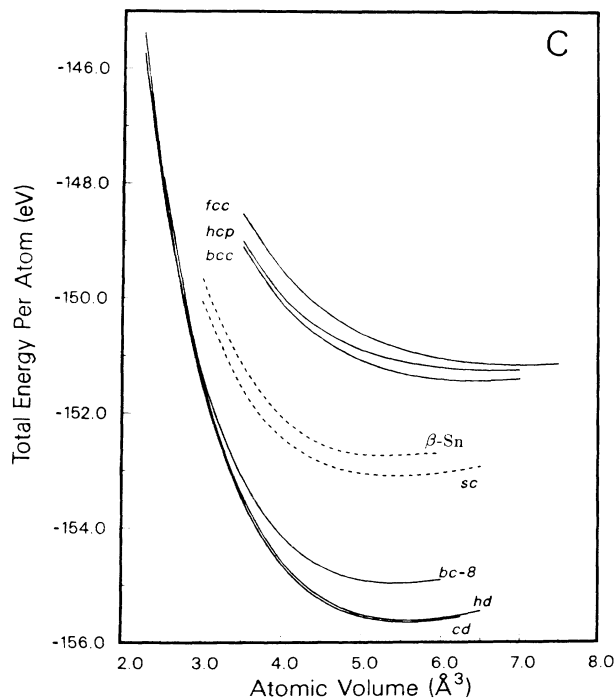


FIG. 1. Calculated total energy vs atomic volume for the eight structures included in this study. The structures are cubic diamond (cd), hexagonal diamond (hd), bc-8, simple cubic (sc), β -tin (β -Sn), body-centered cubic (bcc), hexagonal close packed (hcp), face-centered cubic (fcc). The curves are cubic spline fits through calculated points.

nal diamond having the higher energy. The bc-8 structure lies 0.69 eV/atom higher than cubic diamond at zero pressure, but at 11.1 Mbar their enthalpies become equal and at higher pressures bc-8 is thermodynamically favored over cubic or hexagonal diamond. This transition pressure is in reasonably good agreement with the previous pseudopotential plane-wave calculations,^{8,9} lying somewhat lower than their result of 12 Mbar. We believe that convergence with respect to the basis for the wave functions and the sampling of the Brillouin zone is substantially more complete in the present calculation and that the small discrepancy between the present calculation and those of Refs. 8 and 9 can be attributed to these factors. The compressibility of the bc-8 structure at zero pressure is slightly larger than that of the diamond structures.

We find that the two sixfold coordinated structures, simple cubic and β -tin, are not metastable at low pressure. Both spontaneously transform into the cubic diamond structure without an inhibiting energy barrier. According to the results of Ref. 9, the simple cubic is ultimately favored over the bc-8 structure at 27 Mbar, but in this work we have not investigated the structural properties in that highly compressed regime. The structures of coordination number greater than six lie much higher in energy again than the sixfold structures, and although presumably the close-packed structures would eventually be the

most stable, we do not expect this to occur until the pressure is much greater than 30 Mbar.

Although the structural properties of cubic and hexagonal diamond are almost identical, their electronic behavior under pressure are quite different. Most notably, the fundamental band gap of cubic diamond increases under pressure but that of hexagonal diamond decreases. Thus the hexagonal diamond structure eventually becomes semimetallic at highly compressed volumes but cubic diamond does not. As we shall see, this difference in behavior can be attributed to the different way in which the antibonding orbitals interact in the interstitial region of the two structures. The gap of bc-8 also decreases with pressure, and so cubic diamond is the only fourfold coordinated structure of the three studied here in which the minimum gap increases with pressure.

The remainder of the paper is organized as follows: In Sec. II we describe in detail the crystal structures mentioned above and the relationships between them. The method of calculation is presented in Sec. III. In Secs. IV and V we present results for the structural and electronic properties, respectively, of the structures considered. The main conclusions of this work are in Sec. VI. Appendix A outlines the method of using crystal point group symmetry to reduce the amount of computation in evaluating two- and three-center integrals. Appendix B discusses the problem of satisfying in the cubic diamond structure the conditions for an "ideal" conduction-band minimum for the tetrahedral structures within the qualitative tight-binding analysis discussed in Sec. V, and Appendix C considers the nature of the bottom of the conduction band in the bc-8 structure.

II. STRUCTURES

In this section we describe in detail the crystal structures considered in this work and the relationship between some of them. Much of the subsequent discussion in the paper depends heavily on a clear understanding of the geometries of the bonds and atoms in the various structures. This is especially true in the case of the electronic properties of the tetrahedrally coordinated structures.

Firstly, let us consider the three tetrahedrally coordinated structures, cubic diamond, hexagonal diamond, and the bc-8 structure. Cubic diamond is the commonly occurring form of diamond.²¹ The Bravais lattice is face-centered cubic with two atoms in the unit cell at $\pm a(\frac{1}{8}, \frac{1}{8}, \frac{1}{8})$ in Cartesian coordinates. The space group is O_h^7 . One cubic cell of the structure is shown in Fig. 2. Each atom has four nearest neighbors, with the neighbors situated at the corners of a regular tetrahedron and the atom at its centroid. In this perfect tetrahedral coordination, all the bonds are the same length and are equivalent in the crystal. The angle between any two bonds on an atom is $\cos^{-1}(-\frac{1}{3})=109.47^\circ$. The formation of these strong sp^3 tetrahedral covalent bonds is what gives the diamond structure its exceptional strength. The structure can also be viewed as a set of layers of buckled hexagonal rings of atoms stacked in $\cdots [ABC] \cdots$ sequence in the [111] direction.

This latter view of the cubic diamond structure natural-

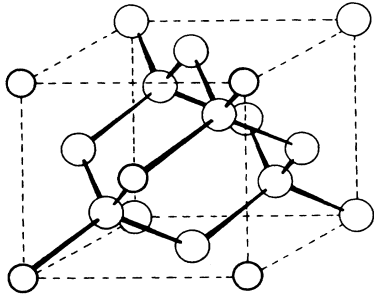


FIG. 2. One cubic unit cell of the cubic diamond structure. The dashed lines show the directions of the cubic axes. The origin of the text description lies half-wave between the two atoms at the lower left corner.

ly leads us to consideration of the hexagonal diamond structure, by analogy with the relationship which exists between the two close-packed structures, face-centered cubic, and hexagonal close packed. Recall that in the fcc structure trigonal planes of atoms are stacked in the $[111]$ direction in $\cdots[ABC]\cdots$ sequence, while the hcp structure consists of trigonal planes stacked in the c direction in $\cdots[AB]\cdots$ sequence. Both structures have the same arrangement of twelve nearest neighbors and only differ in the arrangement of third-nearest neighbors. The hexagonal diamond structure is related to the hcp structure in exactly the same way as cubic diamond is related to the fcc structure; each atom in the hcp structure is replaced by a pair of atoms with the line joining the pair lying in the c direction and of length equal to $\frac{3}{4}$ the inter-layer separation of the hcp structure. In this way perfect tetrahedral coordination of nearest neighbors can be achieved, just as in the cubic diamond structure (see Fig. 3). Again we have layers of buckled hexagonal rings of atoms, but now the stacking is in $\cdots[AB]\cdots$ sequence in the c direction. The unit cell is hexagonal with four atoms in the basis at positions $\pm\{\frac{1}{3}\mathbf{a}_1 + \frac{1}{3}\mathbf{a}_2 + z\mathbf{c}\}$ and $\pm\{\frac{1}{3}\mathbf{a}_1 + \frac{1}{3}\mathbf{a}_2 + (\frac{1}{2}-z)\mathbf{c}\}$, where the angle between the hexagonal basis vectors \mathbf{a}_1 and \mathbf{a}_2 in the basal plane equals $\pi/3$ and c is normal to the basal plane. The space group

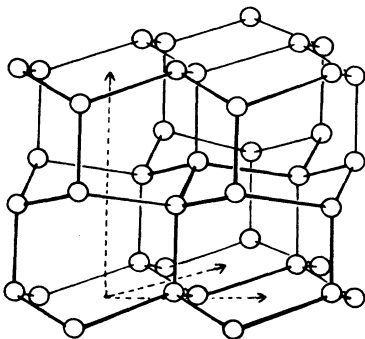


FIG. 3. Three double layers of the hexagonal diamond structure. The primitive basis vectors are the dashed lines. The c direction is vertical and the double-layer stacking is $\cdots[AB]\cdots$ in that direction.

is D_{6h}^4 . Both c/a and z are free parameters from the point of view of crystallographic symmetry. However, perfect tetrahedral coordination is achieved only when $c/a = \sqrt{8/3}$, the ideal ratio for the hcp structure, and $z = \frac{1}{16}$. Cubic and hexagonal diamond are the homopolar analogs of the zinc-blende and wurtzite structures, respectively.

Unlike the two diamond structures, the bc-8 structure does not have perfect tetrahedral coordination; although each atom has four near neighbors, it is connected to one by an A -type bond and to the others by three B -type bonds which may be of slightly different length from the A -type bond. The bond angles are distorted from the ideal tetrahedral angle 109.47° by approximately 10° ($\theta_{A-B} \approx 99^\circ$ and $\theta_{B-B} \approx 117^\circ$). At a given density, the average bond length in the bc-8 structure is greater than in the two diamond structures. Silicon has been synthesized in this structure by releasing pressure from the β -tin structure.¹⁹ The crystallographic description of the structure is as follows: The Bravais lattice is body-centered cubic with eight atoms in the primitive unit cell (hence the notation bc-8) with positions $\pm a(x, -x, x)$, $\pm a(-x, -\frac{1}{2}+x, x)$, $\pm a(\frac{1}{2}-x, -x, -x)$, and $\pm a(x, x, \frac{1}{2}-x)$ in Cartesian coordinates. The side of the cube has length a and x is a free parameter which is approximately equal to $\frac{1}{10}$ for quasitetrahedral coordination. The space group is T_7^h . The ratio r_A/r_B of the bond lengths and the bond angles are determined by displacement parameter x . The distortion of the angles from tetrahedral is an increasing function of x , while $r_A < r_B$ for $x < 0.1036$ and $r_A > r_B$ for $x > 0.1036$. As with the two forms of diamond, this structure can also be viewed as layers of buckled hexagonal rings, although in this case the rings are not regular hexagons. The layers are stacked in $\cdots[AB]\cdots$ sequence in the direction of the cubic axes. A view of two such layers projected down one of the cubic axes is shown in Fig. 4. The numbers in the atoms denote the height above the xy plane in units of $a/10$ for $x = \frac{1}{10}$.

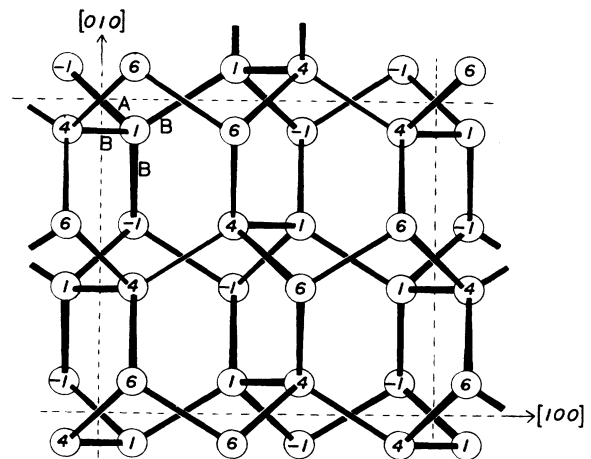


FIG. 4. A projection of two double layers of the bc-8 structure down the $[001]$ axis. The $[100]$ and $[010]$ axes are shown as dashed lines. The numbers in the atoms indicate the height of the atoms above the (001) plane in units of $a/10$ for a value of the internal displacement parameter x equal to $\frac{1}{10}$. There are two inequivalent types of bond, labeled A and B .

Turning now to the sixfold coordinated structures, we firstly consider the simple cubic structure. The structure itself is trivial and needs no description here. However, there is a simple geometrical connection between the simple cubic and cubic diamond structures. Both structures can be described as fcc lattices with a basis of two atoms. The difference between the two is that while the diamond structure has the atoms at $\pm a(\frac{1}{8}, \frac{1}{8}, \frac{1}{8})$, in simple cubic they are at $\pm a(\frac{1}{4}, \frac{1}{4}, \frac{1}{4})$. When described in this fashion, simple cubic is seen as the homopolar analogue of the rocksalt structure.² Thus we can transform simple cubic into the diamond structure through a sequence of fcc lattices with the two atoms in the basis at $\pm a(x, x, x)$. We will calculate the variation of the total energy along this transformation path for one particular atomic volume close to the equilibrium atomic volume for diamond.

The β -tin structure can be obtained from the cubic diamond structure by a simple scaling of all lengths along one of the cubic axes.²¹ For the ideal β -tin structure (i.e., for perfect sixfold coordination), the scaling factor is such that the nearest atoms along the direction of the scaled cubic axis lie the same distance from an atom as the four nearest neighbors of the diamond structure (see Fig. 2). The standard crystallographic description of the structure is²¹ body-centered tetragonal, two atoms in the primitive unit cell at positions $\pm(0, \frac{1}{4}, \frac{3}{8})$ referred to the tetragonal axes, and space group D_{4h}^{14} . The diamond structure then appears as the special case of this structure for which $c/a = \sqrt{2}$ and perfect sixfold coordination occurs for $c/a = 2/\sqrt{15} \simeq 0.516$. We shall see that, unlike the other group-IV elements, silicon, germanium, and tin, no local minimum of the structural energy as a function of c/a occurs near sixfold coordination for carbon at densities near the equilibrium density of diamond; i.e., we obtain no metastable sixfold coordinated structure for carbon.

We will not describe here the higher coordinated structures bcc, hcp, and fcc considered in this study. In the case of the hcp structure we have used the ideal c/a ratio, so that we have perfect twelfold coordination.

III. CALCULATION

The total energy is calculated within local-density-functional theory^{14,18} using the formalism of Ihm *et al.*²⁴ The electron-ion interaction is determined using *ab initio* pseudopotentials generated by the scheme of Hamann, Schluter, and Chiang¹⁵ and the exchange-correlation energy is evaluated with the function of Hedin and Lundqvist.²⁵ We express the total energy as a sum of terms:

$$E_{\text{tot}} = E_{c-c} + E_{\text{kin}} + E_{e-c} + E_{e-e}, \quad (1)$$

where E_{c-c} is the core-core Coulomb interaction (Ewald term), E_{kin} is the kinetic energy of the electrons, E_{e-c} is the electron-core interaction (determined using the ion pseudopotential), and E_{e-e} is the electron-electron interaction (Hartree and exchange correlation).

We determine $E_{\text{kin}} + E_{e-c} + E_{e-e}$ as follows: The Kohn-Sham equations,¹⁸

$$\left[-\frac{\hbar^2}{2m} \nabla^2 + V_{\text{ion}}(\mathbf{r}) + V_H(\mathbf{r}) + \mu_{\text{xc}}(\mathbf{r}) \right] \psi_i(\mathbf{r}) = \epsilon_i \psi_i(\mathbf{r}) \quad (2)$$

are solved self-consistently. Here, V_{ion} is the sum of the ion pseudopotentials, V_H is the Hartree potential due to the valence charge density,

$$\rho(\mathbf{r}) = e \sum_{(\epsilon_i < E_F)} |\psi_i(\mathbf{r})|^2, \quad (3)$$

where E_F is the Fermi level, and $\mu_{\text{xc}}(\mathbf{r})$ is the exchange-correlation potential for the charge density $\rho(\mathbf{r})$. The sum of the electron kinetic, electron-core, and electron-electron energies is given by

$$E_{\text{kin}} + E_{e-c} + E_{e-e} = \sum_{(\epsilon_i < E_F)} \epsilon_i - \frac{1}{2} \int V_H(\mathbf{r}) \rho(\mathbf{r}) d\mathbf{r} + \int [\epsilon_{\text{xc}}(\mathbf{r}) - \mu_{\text{xc}}(\mathbf{r})] \rho(\mathbf{r}) d\mathbf{r}, \quad (4)$$

where $\epsilon_{\text{xc}}(\mathbf{r}) \rho(\mathbf{r})$ is the exchange-correlation energy density. Equation (4) correctly accounts for overcounting of the Coulomb interaction between the electrons in the sum of eigenvalues.

The wave functions are expanded in a linear combination of localized orbitals with s and p symmetry centered on the atomic sites¹⁶ of the form

$$f_{alm}(\mathbf{r}) = A_{alm} e^{-\alpha r^2} K_{lm}(\mathbf{r}), \quad (5)$$

where A_{alm} are normalization constants and K_{lm} are cubic harmonics. Twelve orbitals per atom (i.e., three values of α) are used and the values of the radial Gaussian decays α are chosen to minimize the total energy.²⁶ The potential is made fully self-consistent using the scheme of Chan *et al.*¹⁷ with plane-wave components up to an energy of 64 Ry.

For the cubic diamond structure ten special \mathbf{k} points in the irreducible Brillouin zone were used in the calculation of integrations over the Brillouin zone.²⁷ We have used uniform grids of 21, 11, 56, 59, 47, 50, and 47 \mathbf{k} points in the irreducible zone for the hexagonal diamond, bc-8, simple cubic, β -tin, bcc, hcp, and fcc structures, respectively. In the transition from simple cubic to cubic diamond a uniform grid of 44 \mathbf{k} points in the irreducible zone was used.

IV. STRUCTURAL PROPERTIES

In this section we will present the results obtained for the structural total energies for the various structures outlined in Sec. II. The energy as a function of atomic volume for the eight structures is shown in Fig. 1. Each curve is a cubic spline fit through calculated points. Three groups of structures clearly emerge well separated in energy from one another at low pressure: the fourfold coordinated structures, cubic and hexagonal diamond, and the bc-8 structure; the sixfold coordinated structures, simple cubic, and ideal β -tin; and the highly coordinated structures bcc, hcp, and fcc.

Firstly we discuss the fourfold coordinated structures.

TABLE I. Calculated lattice constants, bulk modulus, its pressure derivative, and cohesive energy for cubic diamond, hexagonal diamond, and bc-8.

	a_0 (Å)	c_0 (Å)	B_0 (GPa)	B'_0	E_{coh} (eV/atom)
Cubic diamond					
Present calc.	3.548		444	3.24	8.17
Expt.	3.567 ^a		443 ^b	4 ^c	7.37 ^d
Hexagonal diamond					
Present calc.	2.50	4.14	440	3.5	8.14
Expt. ^e	2.52	4.12			
Expt. ^f	2.51	4.12			
bc-8					
Present calc.	4.436		411	3.7	7.48

^aReference 21.

^bReference 29.

^cEstimated value from Ref. 30.

^dReference 31.

^eReference 32.

^fReference 22.

The equilibrium lattice constants, bulk moduli, and pressure derivative of the bulk moduli are given in Table I. These were calculated by fitting the total energy curve for each structure to the Murnagahn equation of state²⁸ near the equilibrium atomic volume. From the structural point of view, cubic and hexagonal diamond are almost identical. Their calculated equilibrium volumes differ by only 0.2% and their bulk moduli by 1%—within the theoretical uncertainty for these quantities. The calculated structural properties are in extremely good agreement with experiment^{21,22,29–32} for both cubic and hexagonal diamond.

We find cubic diamond more stable than hexagonal diamond at zero pressure by 0.03 eV/atom. This difference has not been measured experimentally. The energy of cubic diamond remains lower than hexagonal diamond at all volumes calculated in this study. The binding energy of cubic diamond includes a zero-point motion energy of 0.18 eV/atom, estimated from the experimental Debye temperature of diamond.¹⁶ We have assumed that the zero-point energies of the hexagonal diamond and bc-8 structures are the same as that of cubic diamond and have included them in the binding energies of those structures. As is usually the case, local-density-functional theory

overestimates the binding energy of the crystal.^{16,33}

For hexagonal diamond the total energy was minimized with respect to c/a and the internal displacement parameter z at fixed atomic volume for volumes for 3 and 5 Å³. At atomic volume equal to 3 Å³, the energy minimum occurs at $c/a=1.690$ and $z=0.066$; for volume 5 Å³, the minimum is at $c/a=1.665$ and $z=0.063$. (For perfect tetrahedral coordination, $c/a=1.633$ and $z=0.0625$.) At other volumes c/a and z were linearly interpolated with respect to volume between these values.

We have also calculated the phonon frequency of the Γ_1 optical phonon mode for hexagonal diamond (associated with variation of the z internal displacement parameter) at the equilibrium volume using the frozen phonon method.¹⁶ We obtain a value of 42.2 THz or 1407 cm⁻¹. This is somewhat higher than the value of 40.1 THz calculated^{10,16} for the corresponding Γ -point optical phonon mode in cubic diamond. Nielsen¹¹ calculated a value of 38.9 THz for this phonon frequency in cubic diamond. The experimental value³⁴ for cubic diamond is 39.96 THz. To our knowledge, this phonon frequency in hexagonal diamond has not been measured.

Turning now to the bc-8 structure, we find that while the enthalpy of this structure is 0.69 eV/atom higher than cubic diamond at zero pressure, as the pressure is increased the difference in the enthalpies becomes smaller, and the bc-8 structure eventually becomes more stable than the cubic diamond at pressures higher than 11.1 Mbar. The transition pressure is equal to minus the slope of the common tangent to the cubic diamond and bc-8 curves in Fig. 1. The initial (diamond) atomic volume at the transition is 0.492 and the final (bc-8) volume is 0.471 of the equilibrium volume for diamond (see Table II). Two earlier pseudopotential plane-wave calculations^{8,9} found a value of 12 Mbar for this transition pressure. We believe the small discrepancy between these results and the present calculation is due to inadequate convergence with respect to Brillouin zone sampling and also (more

TABLE II. Transition pressure and initial (diamond) and final (bc-8) volumes for the transition from cubic diamond to bc-8. The volumes are given as ratios to the measured equilibrium diamond volume.

	Pressure (Mbar)	Initial volume	Final volume
Present calc.	11.1	0.492	0.471
Reference 8	12	a	
Reference 9	12	0.468	0.456

^aThe volume change given in Ref. 8 is 0.011 of the equilibrium diamond volume, but the initial and final volumes are not given.

important) basis size in the earlier calculations. The local orbital basis used in the present calculation is approximately equivalent for structural properties to a plane-wave basis with plane waves up to a kinetic energy of 60 Ry.

In calculating the energy as a function of volume for bc-8, the value of x , the internal displacement parameter, was chosen to minimize the energy at atomic volumes 2.5 and 4 \AA^3 and linearly interpolated with respect to volume for the other volumes. For atomic volume 2.5 \AA^3 , $x=0.1038$ minimizes the energy, and for volume 4 \AA^3 , $x=0.0991$. By varying x about the equilibrium value for these volumes we can calculate the frequency of the Γ_1 optical phonon. We obtain in this way phonon frequencies of 61.8 and 49.4 THz for atomic volumes 2.5 and 4 \AA^3 , respectively.

The question naturally arises as to whether the charge density of these three tetrahedrally coordinated structures all display the usual characteristics of strongly covalently bonded crystals, especially at highly compressed volumes. This question occurs particularly in the case of the hexagonal diamond and bc-8 structures where the fundamental gap decreases with pressure, causing them eventually to become semimetallic. One might expect that this behavior in the electronic structure would be accompanied by a weakening of the bond charge—in accordance with the traditional picture of metallicity being associated with a more uniform charge density. The charge densities in planes containing the bond chains for the three structures are shown in Fig. 5 for atomic volumes equal to approximately $\frac{1}{2}$ the equilibrium volume of diamond. For cubic diamond all the bonds are equivalent and for hexagonal diamond and bc-8 the two inequivalent types of bond are shown. The most amenable to direct comparison are cubic and hexagonal diamond since the arrangement of atoms is the same locally for both structures. Hexagonal diamond is semimetallic at the volume shown but nevertheless shows virtually no sign of weakening of the co-

valent bonds compared with cubic diamond which is insulating with a large gap. The bc-8 structure displays some weakening of the bond and a somewhat higher interstitial charge density but the effect is small.

The simple cubic and ideal β -tin curve in Fig. 1 are shown dashed because we find them to be not metastable at moderate pressures. The simple cubic and cubic diamond structures can both be included as special cases of a more general structure with a fcc Bravais lattice and two atoms in the unit cell at positions $\pm a(x, x, x)$, as described in Sec. II. In Fig. 6 we present the total energy as a function of x for an atomic volume of 5.0 \AA^3 . The curve is symmetrical about $x=0.5$, the simple cubic structure. The simple-cubic structure is a local maximum, not a local minimum as would be required for metastability.

We show in Fig. 7 the total energy of the β -tin structure as a function of c/a , again for atomic volume equal to 5.0 \AA^3 . No local minimum occurs near the sixfold coordinated β -tin. The origin of the stability of β -tin itself for the observed c/a ratio of 0.546 is a very sharp minimum in the Ewald term of the structure as a function of c/a at just this value.³⁵ The Ewald term corresponds to the electrostatic energy of the point ions in a *uniform* negative background. Clearly the physical relevance of such a term is small in a system in which the electronic charge density favors the highly *nonuniform* distribution associated with the formation of a strong covalent bond charge, as is the case in carbon.

This marked instability of the sixfold coordinated crystalline structures suggests that stable or metastable carbon clusters with atomic coordination number greater than four will be unlikely to occur, in contrast to the situation in silicon.³⁶ Indeed, the great differences between the bulk phase diagram presented in Fig. 1 and the corresponding diagram for silicon²⁰ indicate that in general the formation of clusters for carbon will be very different from their formation for silicon. The existence of the very

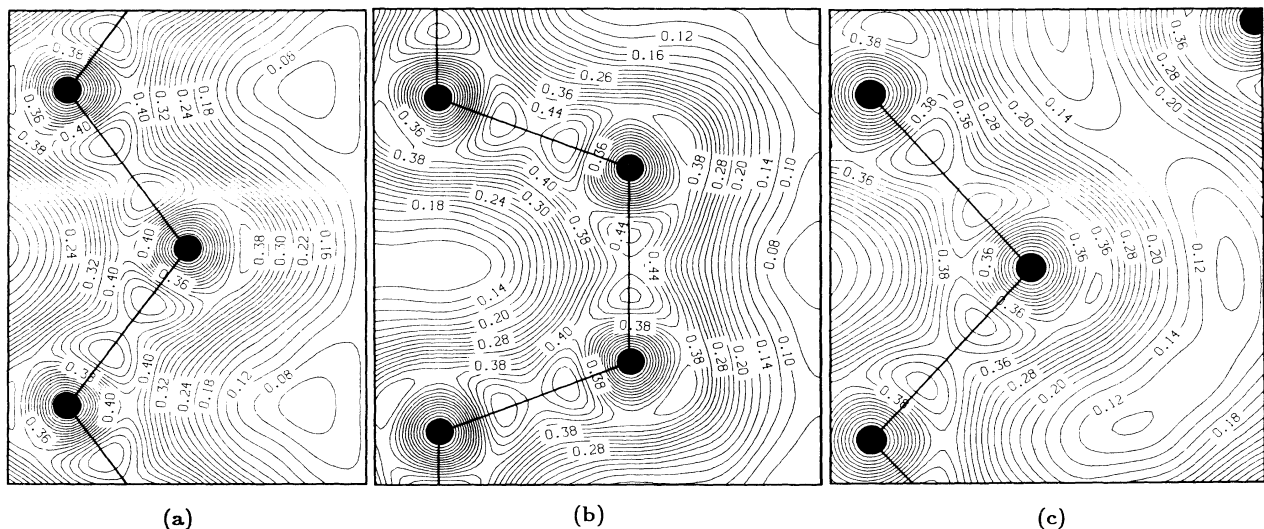


FIG. 5. Charge densities (in atomic units) in planes containing the bond chains for (a) cubic diamond, (b) hexagonal diamond, and (c) bc-8 at atomic volume 2.5 \AA^3 . The positions of the atoms are indicated by solid circles.

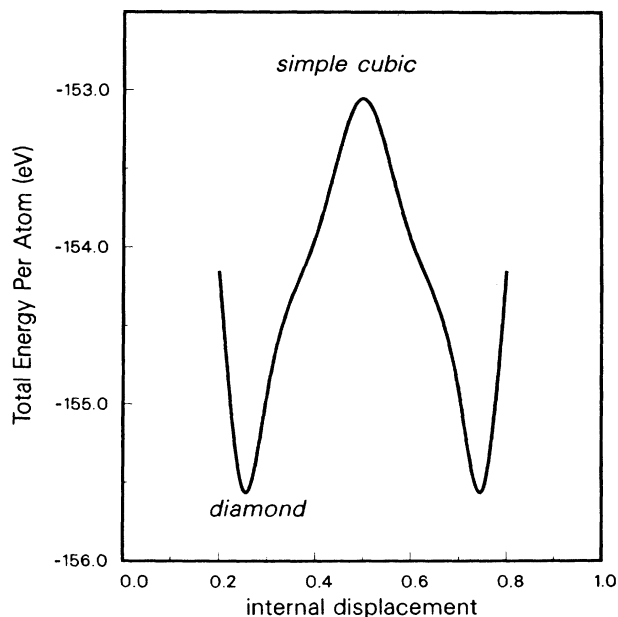


FIG. 6. Calculated total energy vs internal displacement x for the transition from simple cubic to cubic diamond discussed in the text. The atomic volume equals 5.0 \AA^3 . The curve is a cubic spline fit through calculated points.

stable threefold coordinated graphite structure for carbon should also be important for the formation of carbon clusters. For the same reasons, we would not expect to observe sixfold coordination in liquid carbon at moderate temperatures and pressures.

We close this section about structural properties with a qualitative remark about the metastability of the bc-8

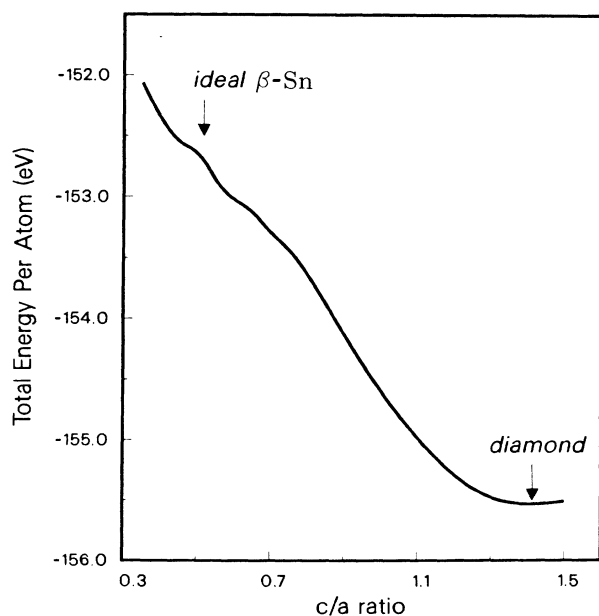


FIG. 7. Calculated total energy for the β -tin structure vs the c/a ratio. The atomic volume equals 5.0 \AA^3 . The curve is a cubic spline fit through calculated points.

structure at low pressure. As can be seen by inspection of Fig. 4, the bc-8 structure can be transformed into the graphite structure by breaking only one bond per pair of atoms, keeping the bonds in the (001) double layers unbroken throughout the transformation. We further note that it has been shown³⁷ that the breaking of the tetrahedral sp^3 bonds in the diamond structure and subsequent formation of the planar sp^2 bonds of the graphite structure can be achieved with an energy barrier of only 0.33 eV per atom. Since the energy of the equilibrium bc-8 structure is 0.7 eV per atom higher than graphite, it seems likely that the transformation of the bc-8 structure into the graphite structure in the manner just mentioned would proceed without an inhibiting energy barrier. This argument suggests that the bc-8 structure would not be metastable for carbon at low pressure, in the contrast to the case for silicon.¹⁹

V. ELECTRONIC PROPERTIES

In this section we will present results for some of the electronic properties of the fourfold coordinated structures and discuss the qualitative features of these properties. In particular, we will be mainly concerned with understanding, in terms of a simple tight-binding picture of the electronic states, the striking differences of behavior in the variation of the fundamental band gap with pressure among these three structures. Although the calculated structural properties of cubic and hexagonal diamond are almost identical, their calculated electronic properties differ in one important respect; viz., in cubic diamond the fundamental gap increases with pressure while in hexagonal diamond it decreases with pressure. At volume compression of 50% from equilibrium, the gap for cubic diamond is approximately 6.5 eV but in hexagonal diamond there is a band overlap of about 2 eV. The band gap of the bc-8 structure also decreases with pressure, eventually leading to semimetallic behavior.

In cubic diamond the fundamental band gap is from Γ to $0.76X$ with a value of 4.3 eV at zero pressure and a pressure derivative of 0.6 meV/kbar in the present calculation.³⁸ Experimentally, the fundamental band gap is from Γ to $0.78X$ ³⁹ with a value of 5.47 eV (Ref. 40) and a pressure derivative of 0.5 meV/kbar (Ref. 41) (see Table III). As is the case in many materials, the band gap is substantially underestimated in local-density-functional

TABLE III. The fundamental band gap E_g at equilibrium and its pressure derivative dE_g/dP for cubic diamond, hexagonal diamond, and bc-8.

	E_g (eV)	dE_g/dP (meV/kbar)
Cubic diamond		
Present calc.	4.3	0.6
Expt.	5.47 ^a	0.5 ^b
Hexagonal diamond	3.3	-1.2
bc-8	2.5	-0.9

^aReference 40.

^bReference 41.

theory compared with experiment but the pressure derivative is approximately correct.^{4,42} In hexagonal diamond the fundamental band gap is from Γ to K with a value of 3.3 eV and a pressure derivative of -1.2 meV/kbar in the present calculation. To our knowledge, the band gap of hexagonal diamond has not been measured experimentally. The fundamental gap is direct at H in the bc-8 structure and has a value of 2.5 eV at equilibrium volume and a pressure derivative of -0.9 meV/kbar. At the transition pressure of cubic diamond to bc-8 the latter structure has a band overlap of 2.5 eV.

The top of the valence band (at Γ) which is triply degenerate in cubic diamond splits into a singly degenerate state and a doubly degenerate manifold when we go to hexagonal diamond. This splitting is caused by the inequivalence of the bond along the c direction to the bonds in the (0001) double layers and is not very large (≈ 1 eV). In bc-8 the top of the valence band (at H) is triply degenerate. (Recall that the H point has the full symmetry of the crystal in the bcc bravais lattice.) The existence of such triply degenerate states at the top of the valence band for general tetrahedrally coordinated networks has been discussed by Ziman.⁴³ We will discuss the reason for the valence band maximum being at H rather than Γ for the bc-8 structure in Appendix C.

When considered as tetrahedrally coordinated networks, the difference between the valence band properties of the three structures are not great. This is hardly surprising since their structural properties are very similar, especially for the two diamond structures. However, the conduction bands differ significantly among the three structures. It is the differences in the conduction bands which are largely responsible for the different behavior of the band gaps. In what follows we will provide a simple qualitative understanding of states at the bottom of the conduction band in the hexagonal diamond and bc-8 structures and see why their behavior is different from the states at the bottom of the conduction band in cubic diamond.

If we think in terms of a very crude tight-binding analysis and consider the conduction bands as composed mainly of sp^3 antibonding orbitals (one for each bond of the structure) concentrated largely in the region behind each bond with a node in the center of the bond, the following qualitative picture emerges of the low-lying conduction states: If we wish the energy of the state to be as low as possible we would like ideally to satisfy the following two conditions.

(1) The state should have mainly p character near each atom (because the bonding-antibonding splitting is much greater for s states than for p states). This means that the sum of the amplitudes of the sp^3 orbitals centered on each atom should equal zero if we wish the energy of the state to be as low as possible. Let us call this condition "the atomic condition" on the wave function for a minimum of the conduction band.

(2) It is intuitively clear that the kinetic energy in the interstitial region of the crystal will be smallest if the antibonding orbitals which interact there combine in phase with one another and with equal amplitudes. (We consider the antibonding orbitals associated with two bonds to

interact in the sense of this condition if the lines pointing in the opposite direction to the bond from each atom are direct at the same point in the interstitial region.) Viewed from the center of the interstitial region, this condition reduces both the angular and radial variation of the wave function and so reduces its kinetic energy. This condition we may call "the interstitial condition" on the wave function for a minimum of the conduction band.

With these two simple conditions in mind, we may then analyze the geometries of the three tetrahedrally coordinated structures and ask which states will satisfy both. As is shown in Appendix B, it is not possible to satisfy both these conditions simultaneously in cubic diamond. Γ_{15} satisfies the right conditions near the atoms but not in the interstitial region, while for Γ_2 the opposite is true. X_1 achieves a compromise for both conditions, satisfying each partially but not entirely. Thus in the case of the cubic diamond structure these two qualitative conditions are indeterminate in identifying the symmetry of the lowest conduction-band state. However, we might expect that a tetrahedrally coordinated structure which can successfully accommodate both conditions for some state would have a smaller band gap.

In the hexagonal diamond structure it does prove possible to satisfy exactly both the "atomic" and "interstitial" conditions simultaneously at the K point. A projection onto the a plane of the state which does so is shown schematically in Fig. 8; the numbers on each bond line give the amplitude of the associated antibonding orbital in the tight binding expansion of the state at the bottom of the conduction band. One layer of bonds is shown in the figure—all other layers have the same projection. The solid circles denote atoms below the plane and the open circles atoms above the plane. Thus if the antibonding orbitals are thought of as being diametrically opposite to the

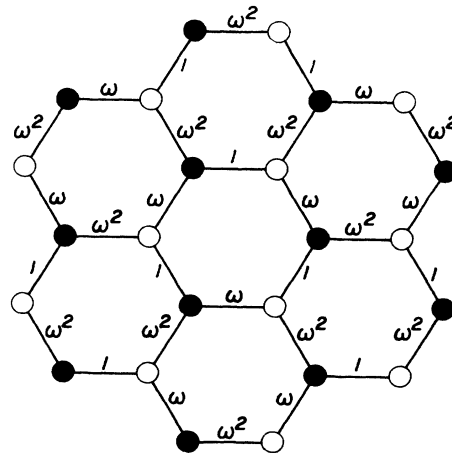


FIG. 8. A projection down the c axis in hexagonal diamond of one double layer of the tight-binding expansion of the state at the conduction band minimum. (See text for details.) The solid circles denote atoms below the (0001) plane and the open circles atoms above the plane. The labels on the bond lines indicate the amplitude of the corresponding antibond in the tight-binding expansion.

bonds on each atom, every second antibond directed into each hexagonal ring points above the plane of the ring and interacts strongly with the other two antibonds pointing above the ring but does not interact strongly with the three antibonds which point below the plane of the ring. The antibonds pointing below the plane of each ring interact with the corresponding antibonds pointing up from the next layer below (see Fig. 3). The eigenstate has the translational symmetry of the K point and even parity with respect to reflection in the horizontal plane which bisects the bonds in the c direction (see Fig. 3). Rotation by $2\pi/3$ about any one of the bonds in the c direction multiplies the state by $\omega = e^{2\pi i/3}$. Thus the state has no weight on the vertical antibond but has amplitudes $1, \omega, \omega^2$ on the other three sp^3 antibonds for each atom. (This prescription uniquely determines the state within our simple tight-binding expansion.) Since $1 + \omega + \omega^2 = 0$, the state has entirely p character near all the atoms so that the atomic condition is perfectly satisfied. Furthermore, as can be seen from Figs. 8 and 3, the antibonding orbitals add perfectly in phase in each interstitial region, and so the interstitial condition is also satisfied.

At the H point in the bc-8 structure it is also possible to create an antibonding state which satisfies the interstitial condition exactly and the atomic condition almost exactly. The nature of this state is discussed in detail in Appendix C. Thus we see qualitatively how the band gap in both hexagonal diamond and bc-8 is substantially smaller than in cubic diamond. The frustration in the cubic diamond structure of the atomic and interstitial conditions for the conduction-band minimum leads to a larger gap. As the structures are compressed, and all the interactions between the antibonds increase in magnitude, the effect of this frustration increases the difference in the conduction-band minimum between the cubic diamond structure and the hexagonal diamond and bc-8 structures, where the frustration is avoided. These arguments do not unambiguously determine the signs of the pressure derivative of the fundamental gap in the three tetrahedrally coordinated phases but only indicate that we can expect a derivative for cubic diamond greater than for the other two structures. The most important point to be made from this discussion is that the conduction band energies depend critically on antibond interaction in the interstitial region.

Finally, we caution that the above analysis is only appropriate for carbon and should not be applied to silicon or germanium where atomic d states play an important role in the conduction bands.³⁸ However, with minor modification the arguments should be applicable to the tetrahedrally coordinated phases of boron nitride. Thus we expect the same differences to occur between BN in the zinc-blende and wurtzite structures.

VI. CONCLUSIONS

In conclusion we have studied the structural properties of eight phases of carbon and also in detail the electronic properties of three fourfold coordinated phases at high pressure, using the pseudopotential local-orbital total energy technique. At pressures below 10 Mbar the fourfold coordinated structures are well removed in enthalpy from

the sixfold coordinated structures which are in turn well removed from the eight and twelfold coordinated structures. The structural properties of cubic and hexagonal diamond are almost identical, with cubic diamond lying very slightly below hexagonal diamond in energy over the entire range of volumes studied here. At pressures greater than 11.1 Mbar bc-8 is more stable than cubic diamond. This transition pressure is slightly lower than earlier calculations have found. At moderate pressures we find the sixfold coordinated structures to be not metastable, transforming spontaneously without an inhibiting energy barrier into the cubic diamond structure. We also suggest that the bc-8 structure for carbon would not be metastable at low pressures, unlike the situation for silicon where it can be obtained by the unloading of Si-II (silicon in the β -tin structure).

Although the structural properties of cubic and hexagonal diamond are almost identical, their electronic behavior under pressure is found to differ significantly. The fundamental band gap in cubic diamond is found to increase under pressure, in agreement with experiment, while that of hexagonal diamond is predicted to decrease. Cubic diamond remains insulating with a large band gap at very high pressure while hexagonal diamond eventually becomes semimetallic. The bc-8 structure also exhibits this semimetallic behavior under pressure. We have proposed two simple conditions within a tight-binding picture for an ideal conduction-band minimum in quasitrahedrally coordinated carbon which provide qualitative understanding of the surprising differences in behavior between cubic diamond and the other two fourfold coordinated structures.

ACKNOWLEDGMENTS

We gratefully acknowledge many helpful discussions with C. T. Chan, M. S. Hybertsen, and R. M. Wentzcovitch. This work has been supported by National Science Foundation Grant No. DMR8319024 and by the Director, Office of Energy Research, Office of Basic Energy Sciences, Materials Sciences Division of the U.S. Department of Energy under Contract No. DE-AC03-76SF00098. We also acknowledge a National Science Foundation supercomputer time grant at Purdue University Computing Center. One of us (S.F.) wishes to thank the National University of Ireland for financial support during the early stages of this work. One of us (S.G.L.) acknowledges support from the Miller Institute.

APPENDIX A

In this appendix we outline a method of utilizing the crystal space-group symmetry to the full in reducing the computational effort involved in evaluating two- and three-center integrals in the Hamiltonian and overlap matrix elements. Smith, Gay, and Arlinghaus⁴⁴ have used crystal symmetry in essentially the same way to evaluate two-center integrals for the special case of the Cu(100) surface. Here we will present the formulation of the approach for crystals with arbitrary space groups (symmorphic or nonsymmorphic). Furthermore, we will see that substantial further saving in computation can be

achieved by making use of the special form of the initial (non-self-consistent) crystal potential as a sum of spherically symmetric potentials centered on the ion sites¹⁶ (viz., in evaluating three-center integrals). The evaluation of two- and three-center integrals is a very computationally intensive aspect of the local-orbital approach and so the optimum utilization of the crystal symmetry in reducing this effort is clearly of considerable practical importance.

Let $|\alpha lm \mathbf{r}_0\rangle$ denote the local-orbital basis function which has coordinate representation $A_{alm} e^{-\alpha(r-\mathbf{r}_0)^2} \times K_{lm}(\mathbf{r}-\mathbf{r}_0)$, where K_{lm} are the cubic harmonics and A_{alm} are normalization constants.¹⁶ Let \mathcal{T} be any Euclidean transformation defined by

$$\mathcal{T}:\mathbf{r} \mapsto T\mathbf{r}-\boldsymbol{\tau}, \quad (\text{A1})$$

where T is an orthogonal transformation (the rotational part of \mathcal{T}) and $\boldsymbol{\tau}$ is a vector (the translational part of \mathcal{T}). Each \mathcal{T} induces an action, $\Theta_{\mathcal{T}}$, on the space of wave functions in the usual manner; viz., in coordinate representation

$$\Theta_{\mathcal{T}}:f(\mathbf{r}) \mapsto f(\mathcal{T}^{-1}\mathbf{r}). \quad (\text{A2})$$

$$\begin{aligned} \langle \alpha_1 l_1 m_1 \mathbf{r}_1 | \Theta_{\mathcal{T}}^{-1} O' \Theta_{\mathcal{T}} | \alpha_2 l_2 m_2 \mathbf{r}_2 \rangle &= \{ \langle \alpha_1 l_1 m_1 \mathbf{r}_1 | \Theta_{\mathcal{T}}^* \} O' \{ \Theta_{\mathcal{T}} | \alpha_2 l_2 m_2 \mathbf{r}_2 \rangle \} \\ &= \left[\sum_{m'_1} \langle \alpha_1 l_1 m'_1 \mathbf{r}'_1 | \Lambda_{m'_1 m_1}^{l_1}(T)^* \right] O' \left[\sum_{m'_2} \Lambda_{m'_2 m_2}^{l_2}(T) | \alpha_2 l_2 m'_2 \mathbf{r}'_2 \rangle \right] \\ &= \sum_{m'_1, m'_2} \Lambda_{m'_1 m_1}^{l_1}(T)^* \langle \alpha_1 l_1 m'_1 \mathbf{r}'_1 | O' | \alpha_2 l_2 m'_2 \mathbf{r}'_2 \rangle \Lambda_{m'_2 m_2}^{l_2}(T), \end{aligned} \quad (\text{A6})$$

where $\mathbf{r}'_1 = \mathcal{T}\mathbf{r}_1$ and $\mathbf{r}'_2 = \mathcal{T}\mathbf{r}_2$. Thus we see that the matrix elements for the operator O between the sites \mathbf{r}_1 and \mathbf{r}_2 are simple linear combinations of the matrix elements for O' between sites \mathbf{r}'_1 and \mathbf{r}'_2 . Combining Eqs. (A5) and (A6) and writing the result in the obvious matrix notation, we obtain

$$\begin{aligned} O(\alpha_1 l_1 \mathbf{r}_1; \alpha_2 l_2 \mathbf{r}_2) \\ = [\Lambda^{l_1}(T)]^* O'(\alpha_1 l_1 \mathbf{r}'_1; \alpha_2 l_2 \mathbf{r}'_2) \Lambda^{l_2}(T), \end{aligned} \quad (\text{A7})$$

or conversely,

$$O'(\alpha_1 l_1 \mathbf{r}'_1; \alpha_2 l_2 \mathbf{r}'_2) = \Lambda^{l_1}(T) O(\alpha_1 l_1 \mathbf{r}_1; \alpha_2 l_2 \mathbf{r}_2) \Lambda^{l_2}(T)^*. \quad (\text{A8})$$

We can now apply Eq. (A8) to the particular case when O is the Hamiltonian and \mathcal{T} belongs to the crystal space group. In that case $O' = O$, since $\Theta_{\mathcal{T}}$ commutes with O , and we see that the Hamiltonian matrix elements between the sites \mathbf{r}'_1 and \mathbf{r}'_2 are simple linear combinations of those between \mathbf{r}_1 and \mathbf{r}_2 . The same is true of the overlap matrix elements. Usually one makes use only of the pure translation group of the crystal in Eq. (A8)—a trivial application of the result, since $\Lambda \equiv 1$ in that case. In this way \mathbf{r}_1 is restricted to be in one unit cell while \mathbf{r}_2 varies over all the neighbors of \mathbf{r}_1 . However, if we go further and use the full space group of the crystal, we can generate $H(\alpha_1 l_1 \mathbf{r}'_1; \alpha_2 l_2 \mathbf{r}'_2)$ from Eq. (A8) for $|G|/|G(\mathbf{r}_1, \mathbf{r}_2)|$ pairs, $(\mathbf{r}'_1, \mathbf{r}'_2)$, from every $H(\alpha_1 l_1 \mathbf{r}_1; \alpha_2 l_2 \mathbf{r}_2)$ calculated. [Here G is the point group

It follows directly from the angular form of the cubic harmonics that

$$\Theta_{\mathcal{T}} |\alpha lm \mathbf{r}_0\rangle = \sum_{m'} \Lambda_{m'm}^{l}(T) |\alpha lm' \mathbf{r}'_0\rangle, \quad (\text{A3})$$

where $\mathbf{r}'_0 = \mathcal{T}\mathbf{r}_0$, and Λ^l is a $(2l+1) \times (2l+1)$ matrix which depends only on T , the rotational part of \mathcal{T} , not the translational part. For $l=0$, $\Lambda=1$ for all T , and for $l=1$, Λ is simply the usual matrix representation of T with respect to the Cartesian axes.

The overlap and Hamiltonian matrix elements we need to evaluate (i.e., the two-center integrals) are of the form,

$$\langle \alpha_1 l_1 m_1 \mathbf{r}_1 | O | \alpha_2 l_2 m_2 \mathbf{r}_2 \rangle, \quad (\text{A4})$$

where O is the identity operator or the Hamiltonian, respectively. We now observe that, for any operator O and any \mathcal{T} ,

$$\begin{aligned} \langle \alpha_1 l_1 m_1 \mathbf{r}_1 | O | \alpha_2 l_2 m_2 \mathbf{r}_2 \rangle \\ = \langle \alpha_1 l_1 m_1 \mathbf{r}_1 | \Theta_{\mathcal{T}}^{-1} O' \Theta_{\mathcal{T}} | \alpha_2 l_2 m_2 \mathbf{r}_2 \rangle, \end{aligned} \quad (\text{A5})$$

where $O' = \Theta_{\mathcal{T}} O \Theta_{\mathcal{T}}^{-1}$. Since Θ is a unitary representation of the Euclidean group, then $\Theta_{\mathcal{T}}^{-1} = \Theta_{\mathcal{T}}^*$. Therefore,

of the crystal and $G(\mathbf{r}_1, \mathbf{r}_2)$ is the subgroup of G which leaves \mathbf{r}_1 and \mathbf{r}_2 fixed. $|G|$ is the number of elements in the group G .] Since the computation involved in generating $H(\alpha_1 l_1 \mathbf{r}'_1; \alpha_2 l_2 \mathbf{r}'_2)$ from Eq. (A8) is negligible compared to that in evaluating $H(\alpha_1 l_1 \mathbf{r}_1; \alpha_2 l_2 \mathbf{r}_2)$, we save a factor of approximately $|G|/|G(\mathbf{r}_1, \mathbf{r}_2)|$ by utilizing the full space group symmetry rather than translational symmetry only.

When $|G(\mathbf{r}_1, \mathbf{r}_2)|$ is greater than one, it is possible to reduce the amount of computation involved in calculating $H(\alpha_1 l_1 \mathbf{r}_1; \alpha_2 l_2 \mathbf{r}_2)$ itself. To do so we consider the particular form of the crystal Hamiltonian,

$$H = \sum_{\mathbf{R}, i} V_{\mathbf{R}+\boldsymbol{\tau}_i}^i + \frac{\hbar^2}{2m} \nabla^2. \quad (\text{A9})$$

Here \mathbf{R} are the crystal lattice vectors, $\boldsymbol{\tau}_i$ are the positions of the ions within the unit cell, and $V_{\mathbf{r}}^i$ is the total potential (local and nonlocal) due to the ion (of type i) at position \mathbf{r} . Thus H is expressed as a sum of spherically symmetric potentials at the ion sites, plus the kinetic energy term. In evaluating the matrix elements of H , we use the form

$$\begin{aligned} \langle \alpha_1 l_1 m_1 \mathbf{r}_1 | H | \alpha_2 l_2 m_2 \mathbf{r}_2 \rangle \\ = \sum_{\mathbf{R}, i} \langle \alpha_1 l_1 m_1 \mathbf{r}_1 | V_{\mathbf{R}+\boldsymbol{\tau}_i}^i | \alpha_2 l_2 m_2 \mathbf{r}_2 \rangle \\ + \left\langle \alpha_1 l_1 m_1 \mathbf{r}_1 \left| \frac{\hbar^2}{2m} \nabla^2 \right| \alpha_2 l_2 m_2 \mathbf{r}_2 \right\rangle, \end{aligned} \quad (\text{A10})$$

For each individual \mathbf{r} , $\langle \alpha_1 l_1 m_1 \mathbf{r}_1 | V_r^i | \alpha_2 l_2 m_2 \mathbf{r}_2 \rangle$ is evaluated, and then the total crystal potential matrix element is obtained from the sum in Eq. (A10). (The kinetic energy matrix element is evaluated separately.) The major computational effort is involved in the evaluation of the three-center integrals $\langle \alpha_1 l_1 m_1 \mathbf{r}_1 | V_r^i | \alpha_2 l_2 m_2 \mathbf{r}_2 \rangle$, since there are many values of \mathbf{r} to be summed for each pair $(\mathbf{r}_1, \mathbf{r}_2)$. Now we can consider Eq. (A8) when \mathcal{T} leaves both \mathbf{r}_1 and \mathbf{r}_2 fixed and let $O = V_r^i$. Then, since V^i is spherically symmetric,

$$O' = \Theta_{\mathcal{T}} V_r^i \Theta_{\mathcal{T}}^{-1} = V_{r'}^i, \quad (\text{A11})$$

where $\mathbf{r}' = \mathcal{T} \cdot \mathbf{r}$. Thus Eq. (A8) becomes

$$V_r^i(\alpha_1 l_1 \mathbf{r}_1; \alpha_2 l_2 \mathbf{r}_2) = \Lambda^l(T) V_{r'}^i(\alpha_1 l_1 \mathbf{r}_1; \alpha_2 l_2 \mathbf{r}_2) [\Lambda^l(T)]^* . \quad (\text{A12})$$

Making use of Eq. (A12), we can generate all the three-center integrals for $|G(\mathbf{r}_1, \mathbf{r}_2)| / |G(\mathbf{r}_1, \mathbf{r}_2, \mathbf{r})|$ values of \mathbf{r}' given those for \mathbf{r} . [$G(\mathbf{r}_1, \mathbf{r}_2, \mathbf{r})$ is the subgroup of G which leaves \mathbf{r}_1 , \mathbf{r}_2 , and \mathbf{r} fixed].

Thus we save a factor of $|G(\mathbf{r}_1, \mathbf{r}_2)| / |G(\mathbf{r}_1, \mathbf{r}_2, \mathbf{r})|$ in evaluating the three-center integrals. Since $|G(\mathbf{r}_1, \mathbf{r}_2, \mathbf{r})|$ is very rarely greater than one and since most of the computation of the Hamiltonian and overlap matrix elements is involved in evaluating these three-center integrals, an overall reduction factor in computation equal to $|G|$, the size of the point group, is achieved by using the full crystal space group instead of just the pure translations.

APPENDIX B

In this appendix we show that it is not possible to satisfy simultaneously both conditions outlined in Sec. V for an ideal conduction band minimum in the cubic diamond structure. As we shall see, the main reason this is not possible in the cubic diamond structure while it is possible in the very similar hexagonal diamond structure is because all four of the antibonds in cubic diamond interact both at the atoms and also in the interstitial region (at the center of the "adamantine cage"). This imposes too many algebraic conditions for a solution to exist. In hexagonal diamond the antibond in the c direction is inequivalent to the other three on the atom and interacts in the interstitial region only with the similar antibond on the neighboring layer (see Fig. 3).

In the cubic diamond structure there are four bonds per unit cell and so we have four antibond amplitudes for any conduction band state within the tight-binding picture. In each primitive unit cell there are two atomic positions and two "tetrahedral" interstitial positions. The interstitial positions are located relative to each atom in positions diametrically opposite the neighboring atoms. Thus each atom is at the body center of a cube which has neighboring atoms at four corners and interstitial sites at the other four diametrically opposite corners. In the description of the cubic diamond lattice in Sec. II, the two atoms in the primitive unit cell are at positions $\pm(\frac{1}{8}, \frac{1}{8}, \frac{1}{8})$ and the two interstitial sites are at $\pm(\frac{3}{8}, \frac{3}{8}, \frac{3}{8})$ (see Fig. 2). (We use Cartesian coordinates throughout this appendix and assume that the cubic cell has sides of unit length.) Four

antibonds interact at each interstitial site.

Let α_i , $i=1,2,3,4$, be the amplitudes of the antibonds associated with the bonds which point from the atom at $(\frac{1}{8}, \frac{1}{8}, \frac{1}{8})$ in the directions $[\bar{1}\bar{1}\bar{1}]$, $[\bar{1}11]$, $[1\bar{1}1]$, and $[11\bar{1}]$, respectively. We define the crystal momentum of the Bloch state as follows: Translation by $[0\frac{1}{2}\frac{1}{2}]$ multiplies the state by θ_2 ; translation by $[\frac{1}{2}0\frac{1}{2}]$ multiplies the state by θ_3 ; translation by $[\frac{1}{2}\frac{1}{2}0]$ multiplies the state by θ_4 ; for notational convenience we define $\theta_1 \equiv 1$. Obviously, for a Bloch state,

$$|\theta_i| = 1 \quad \text{for } i=1,2,3,4 . \quad (\text{B1})$$

The atomic condition for the atom at $(\frac{1}{8}, \frac{1}{8}, \frac{1}{8})$ is then

$$\alpha_1 + \alpha_2 + \alpha_3 + \alpha_4 = 0 . \quad (\text{B2})$$

If we think of the α_i as vectors in the complex plane, Eq. (B2) amounts to the geometric condition that they form the sides of a directed closed quadrilateral. Similarly, the atomic condition for the atom at $(-\frac{1}{8}, -\frac{1}{8}, -\frac{1}{8})$ is

$$-\frac{\alpha_1}{\theta_1} - \frac{\alpha_2}{\theta_2} - \frac{\alpha_3}{\theta_3} - \frac{\alpha_4}{\theta_4} = 0 . \quad (\text{B3})$$

The interstitial condition at $(\frac{3}{8}, \frac{3}{8}, \frac{3}{8})$ is

$$\alpha_1 \theta_1 = \alpha_2 \theta_2 = \alpha_3 \theta_3 = \alpha_4 \theta_4 , \quad (\text{B4})$$

and the condition at $(-\frac{3}{8}, -\frac{3}{8}, -\frac{3}{8})$ is

$$-\frac{\alpha_1}{\theta_1^2} = -\frac{\alpha_2}{\theta_2^2} = -\frac{\alpha_3}{\theta_3^2} = -\frac{\alpha_4}{\theta_4^2} . \quad (\text{B5})$$

Combining Eqs. (B1) and (B4) gives that

$$|\alpha_1| = |\alpha_2| = |\alpha_3| = |\alpha_4| . \quad (\text{B6})$$

Now the geometric interpretation of Eq. (B2) is strengthened to the statement that the α_i form the sides of a rhombus, and so we must have the $\alpha_i = -\alpha_1$, for one of $i=2, 3$, or 4 . Without loss of generality we can assume that $\alpha_2 = -\alpha_1$. The first part of Eq. (B4) then gives us that

$$\theta_2 = -1 . \quad (\text{B7})$$

On the other hand, dividing Eq. (B4) by Eq. (B5) we obtain

$$\theta_i^3 = 1 \quad \text{for } i=2,3,4 . \quad (\text{B8})$$

Clearly, Eq. (B7) contradicts Eq. (B8) and so we cannot construct a Bloch state which simultaneously satisfies both the atomic and the interstitial condition in the cubic diamond structure.

APPENDIX C

In this appendix we discuss the nature of the state at the bottom of the conduction band in the bc-8 structure. The state has the translational symmetry of the H point for the following reason: The A -type antibond from $(-x, x, -x)$ to $(x, -x, x)$ has a very strong interaction with the corresponding bond at the center of the cubic cell, from $(\frac{1}{2}-x, -\frac{1}{2}+x, \frac{1}{2}-x)$ to $(\frac{1}{2}+x, -\frac{1}{2}-x, \frac{1}{2}+x)$

(see Fig. 4). [The four atoms at $(-x, x-x)$, $(x, -x, x)$, $(\frac{1}{2}-x, -\frac{1}{2}+x, \frac{1}{2}-x)$, and $(\frac{1}{2}+x, -\frac{1}{2}-x, \frac{1}{2}+x)$ lie in a straight line and the distance from $(x, -x, x)$ to $(\frac{1}{2}-x, -\frac{1}{2}+x, \frac{1}{2}-x)$ is only approximately $\frac{3}{2}$ times the A -bond length.] For the antibond from $(-x, x, -x)$ to $(x, -x, x)$ to add in phase in the interstitial region with the antibond from $(\frac{1}{2}-x, -\frac{1}{2}+x, \frac{1}{2}-x)$ to $(\frac{1}{2}+x, -\frac{1}{2}-x, \frac{1}{2}+x)$, the state must be multiplied by a factor of -1 when translated by the lattice vector $(\frac{1}{2}, -\frac{1}{2}, \frac{1}{2})$. Similarly, the A -type antibonds from $(-x, -\frac{1}{2}-x, x)$ to $(x, -\frac{1}{2}+x, -x)$ and from $(\frac{1}{2}-x, -x, -\frac{1}{2}+x)$ to $(\frac{1}{2}+x, x, -\frac{1}{2}-x)$ add in phase in the interstitial region only if the state is multiplied by -1 when translated by $(\frac{1}{2}, \frac{1}{2}, -\frac{1}{2})$, and the A -type antibonds from $(\frac{1}{2}+x, -x, -x)$ to $(\frac{1}{2}-x, x, x)$ and from $(x, \frac{1}{2}-x, \frac{1}{2}-x)$ to $(-x, \frac{1}{2}+x, \frac{1}{2}+x)$ add in phase only if the state is multiplied by -1 when translated by $(-\frac{1}{2}, \frac{1}{2}, \frac{1}{2})$. This uniquely determines the translational symmetry of the state as being that of the H point in the Brillouin zone.

Further inspection of the detailed geometry of the bc-8 structure shows that the B -type antibonds have much smaller interaction with each other in the interstitial region (as indicated by their spatial overlap) or with the A -type antibonds than the A -type with other A -type. (The largest overlap is between the B -type antibond from $(\frac{1}{2}+x, -\frac{1}{2}+x, x)$ to $(1-x, -\frac{1}{2}-x, x)$ and the A -type antibond from $(\frac{1}{2}+x, -\frac{1}{2}-x, \frac{1}{2}+x)$ to $(\frac{1}{2}-x, -\frac{1}{2}+x, \frac{1}{2}-x)$, but this is quite small. It transpires that the state which satisfies the atomic condition as well as optimizing the interstitial interaction between the A -type antibonds—in the manner discussed below—also gives the correct (i.e., positive) relative phase between these B - and A -type antibonds for reducing the kinetic energy of a conduction state.)

Because the distance between the atoms at $(x, -x, x)$ and $(\frac{1}{2}-x, -\frac{1}{2}+x, \frac{1}{2}-x)$ is quite small, the combined ionic potential in the region between them is deep. Thus to minimize the energy of the conduction band state at H , we want the amplitude of the antibonds directed at that region (i.e., the A -type antibonds) to be large. In this way

we reduce the potential energy of the state.

We now turn to the atomic condition. The best way to satisfy this (given the requirement that the A -type antibond amplitude be large) is to have the amplitudes on each of the B -type antibonds equal to the others and equal to $-\frac{1}{3}$ the amplitude on the A -type antibond. The symmetry group of the H point ensures that two states of the form

$$\alpha |A^-\rangle + \beta [|B_1^-\rangle + |B_2^-\rangle + |B_3^-\rangle]$$

must exist. (Here $|X^-\rangle$ denotes the antibond corresponding to bond X .) If we assume that the A - B antibond interaction at the atomic site is approximately the same as the B - B antibond interaction, then the two solutions are $\alpha \simeq \beta$ and $\alpha \simeq -3\beta$. The first of these is s -like near the atoms while the second is p -like and is the bottom of the conduction band. Because of the strong interaction between the antibond from $(-x, x, -x)$ to $(x, -x, x)$ and the antibond from $(\frac{1}{2}-x, -\frac{1}{2}+x, \frac{1}{2}-x)$ to $(\frac{1}{2}+x, -\frac{1}{2}-x, \frac{1}{2}+x)$, we have a large dispersion near the bottom of the conduction band; i.e., the conduction band mass is small.

Finally, we remark that the valence band maximum in bc-8 occurs at the H point for essentially the same reason as the conduction band minimum occurs there; viz., the A -type bond in one cell interacts strongly with the corresponding bond in the next cell. At the H point there is a nodal surface on the perpendicular bisector of the line between $(x, -x, x)$ and $(\frac{1}{2}-x, -\frac{1}{2}+x, \frac{1}{2}-x)$ for the Bloch sum of the A -type bond from $(-x, x, -x)$ to $(x, -x, x)$, thus raising its kinetic energy. The states at the top of the valence band transform under the point group like the functions yz , zx , and xy . Each one of these states has exactly zero amplitude on one of the B -type bonds of each atom. The amplitudes on the other two B -type bonds of each atom are approximately equal to one another and equal to $-\frac{1}{2}$ the amplitude on the A -type bond. For states of this kind it is the higher energy of the Bloch sum of the A -type bonds which raises the energy of these states above those at the Γ point.⁴⁵

¹A. Jayaraman, Rev. Mod. Phys. **55**, 65 (1983).

²S. Froyen and M. L. Cohen, Phys. Rev. B **28**, 3258 (1983); **29**, 3770 (1984).

³J. R. Chelikowsky and J. K. Burdett, Phys. Rev. Lett. **56**, 961 (1986).

⁴K. J. Chang, S. Froyen, and M. L. Cohen, Solid State Commun. **50**, 105 (1984).

⁵K. J. Chang, M. M. Dacorogna, M. L. Cohen, J. M. Mignot, G. Chouteau, and G. Martinez, Phys. Rev. Lett. **54**, 2375 (1985).

⁶R. M. Wentzcovitch, K. J. Chang, and M. L. Cohen, Phys. Rev. B **34**, 1071 (1986).

⁷M. T. Yin and M. L. Cohen, Phys. Rev. Lett. **50**, 2006 (1983).

⁸R. Biswas, R. M. Martin, R. J. Needs, and O. H. Nielsen, Phys. Rev. B **30**, 3210 (1984).

⁹M. T. Yin, Phys. Rev. B **30**, 1773 (1984).

¹⁰M. Hanfland, K. Syassen, S. Fahy, S. G. Louie, and M. L.

Cohen, Phys. Rev. B **31**, 6896 (1985); Physica **139**, 516 (1986).

¹¹O. H. Nielsen, Phys. Rev. B **34**, 5808 (1986).

¹²M. Cardona and N. E. Christensen, Solid State Commun. **58**, 421 (1986).

¹³P. E. Van Camp, V. E. Doren, and J. T. Devreese, Phys. Rev. B **34**, 1314 (1986).

¹⁴Theory of the Inhomogeneous Electron Gas, edited by S. Lundqvist and N. H. March (Plenum, New York, 1983), and references therein.

¹⁵D. R. Hamann, M. Schlüter, and C. Chiang, Phys. Rev. Lett. **43**, 1494 (1979).

¹⁶J. R. Chelikowsky and S. G. Louie, Phys. Rev. B **29**, 3470 (1984).

¹⁷C. T. Chan, D. Vanderbilt, and S. G. Louie, Phys. Rev. B **33**, 2455 (1985).

¹⁸P. Hohenberg and W. Kohn, Phys. Rev. **136**, B864 (1964); W. Kohn and L. J. Sham, *ibid.* **140**, A1133 (1965).

- ¹⁹R. H. Wentorf, Jr. and J. S. Kaspar, *Science* **139**, 338 (1963); J. S. Kaspar and S. M. Richards, *Acta Crystallogr.* **17**, 752 (1964).
- ²⁰M. T. Yin and M. L. Cohen, *Phys. Rev. Lett.* **45**, 1004 (1980); and *Solid State Commun.* **38**, 625 (1981).
- ²¹J. Donohue, *The Structures of the Elements* (Krieger, Malabar, Florida, 1982).
- ²²R. E. Hanneman, H. M. Strong, and F. P. Bundy, *Science* **155**, 995 (1967).
- ²³F. P. Bundy and J. S. Kaspar, *J. Chem. Phys.* **46**, 3437 (1967).
- ²⁴J. Ihm, A. Zunger, and M. L. Cohen, *J. Phys. C* **12**, 4409 (1979).
- ²⁵L. Hedin and B. I. Lundqvist, *J. Phys. C* **4**, 2064 (1971).
- ²⁶The values of the radial decays used for all the results presented here were 2.65, 0.797, and 0.24 in atomic units. These decays were chosen to minimize the energy of the cubic diamond structure near its equilibrium lattice constant. (The energy was minimized with respect to the first and last decay, keeping the second decay equal to the geometric mean of the first and last.) Although altering the values of these decays by as much as 40% can change the total energy by up to 0.24 eV/atom, the relative energies of all the structures over the entire range of atomic volumes considered change by less than 0.02 eV/atom. The same can be said for the addition of *d* states to the basis, even for the highly coordinated structures where the inclusion of *d* states might intuitively have been considered important. Thus we can see that the basis set, although small, allows an excellent representation of the valence-band states which determine the structural properties.
- ²⁷D. J. Chadi and M. L. Cohen, *Phys. Rev. B* **8**, 5747 (1973).
- ²⁸F. D. Murnaghan, *Proc. Nat. Acad. Sci. U.S.A.* **3**, 244 (1944). This equation of state assumes that the pressure derivative of the bulk modulus is constant over the range of the fit. In fact the pressure derivative obtained in this way is quite sensitive to the range over which the fit is made. Thus the theoretical uncertainty in this quantity is of the order of 10%. Within this uncertainty, its value for cubic diamond and hexagonal diamond are essentially the same.
- ²⁹H. J. McSkimin and P. Andreatch, Jr., *J. Appl. Phys.* **43**, 985 (1972).
- ³⁰K. Gschneidner, Jr., *Solid State Physics*, edited by F. Seitz, D. Turnbull, and H. Ehrenreich (Academic, New York, 1964), Vol. 16, p. 275.
- ³¹L. Brewer, Lawrence Berkeley Report No. LB-3720, 1977 (unpublished).
- ³²C. Frondel and U. B. Marvin, *Nature* **214**, 587 (1967).
- ³³M. Weinert, E. Wimmer, and A. J. Freeman, *Phys. Rev. B* **26**, 4571 (1982).
- ³⁴As tabulated in J. C. Phillips, *Bonds and Bands in Semiconductors* (Academic, New York, 1973).
- ³⁵M. T. Yin, Ph.D. thesis, University of California, Berkeley, 1982.
- ³⁶D. Tománek and M. Schlüter, *Phys. Rev. Lett.* **56**, 1055 (1986).
- ³⁷S. Fahy, S. G. Louie, and M. L. Cohen, *Phys. Rev. B* **34**, 1191 (1986).
- ³⁸When orbitals with *d* symmetry are included in the local orbital basis the band gap reduces to 3.9 eV and the pressure derivative to 0.53 meV/kbar. For a detailed discussion of the effect of atomic *d* states on the gap of cubic diamond, see, S. Fahy, K. J. Chang, S. G. Louie, and M. L. Cohen, *Phys. Rev. B* **35**, 5856 (1987).
- ³⁹P. J. Dean and E. C. Lightowers, *Phys. Rev.* **140**, A352 (1965).
- ⁴⁰C. D. Clark, P. J. Dean, and P. V. Harris, *Proc. R. Soc. London Ser. A* **277**, 312 (1964).
- ⁴¹*Landolt-Börnstein Tables*, edited by O. Madelung, M. Schulz, and H. Weiss (Springer, Berlin, 1982), Vol. 17a and references therein.
- ⁴²M. S. Hybertsen and S. G. Louie, *Phys. Rev. Lett.* **55**, 1418 (1985); *Phys. Rev. B* **34**, 5390 (1986).
- ⁴³J. M. Ziman, *J. Phys. C* **4**, 3129 (1971).
- ⁴⁴J. R. Smith, J. G. Gay, and F. J. Arlinghaus, *Phys. Rev. B* **21**, 2201 (1980).
- ⁴⁵Note that for $x = \frac{1}{8}$, the energy of the *H*-point Bloch sum of *A*-type bonds is identically equal to the energy of the Bloch sum of *A*-type antibonds. This is because one cannot decide whether the "bond" is between $(-\frac{1}{8}, \frac{1}{8}, -\frac{1}{8})$ and $(\frac{1}{8}, -\frac{1}{8}, \frac{1}{8})$ or between $(\frac{1}{8}, -\frac{1}{8}, \frac{1}{8})$ and $(\frac{3}{8}, -\frac{3}{8}, \frac{3}{8})$.